OncoTargets and Therapy

Dovepress
open access to scientific and medical research

Open Access Full Text Article

ORIGINAL RESEARCH

Potent in vitro and xenograft antitumor activity of a novel agent, PV-10, against relapsed and refractory neuroblastoma

This article was published in the following Dove Medical Press journal:
OncoTargets and Therapy

Lucy Swift[1]
Chunfen Zhang[1]
Tanya Trippett[2]
Aru Narendran[1]

[1]POETIC Laboratory for Preclinical and Drug Discovery Studies, Division of Pediatric Oncology, Alberta Children's Hospital, University of Calgary, Calgary, AB, Canada; [2]Department of Pediatrics, Memorial Sloan-Kettering Cancer Center, New York, NY, USA

Purpose: Neuroblastoma is the most common extracranial cancer in children. Although the prognosis for low-risk neuroblastoma patients is good, the 5-year survival rates for high-risk and relapsed patients are low. The poor survival rates for these patients demonstrate the need for novel therapeutic approaches to treat this disease. PV-10 is a sterile 10% solution of Rose Bengal that has previously been shown to induce cell death in a range of adult cancers, providing the rationale for studying the activity of PV-10 against neuroblastoma in preclinical studies.
Methods: The effects of PV-10 on neuroblastoma were investigated in vitro. Cytotoxicity assays were performed using the alamar blue assay on the following cell lines: SK-N-AS, SK-N-BE(2), IMR5, LAN1, SHEP, and SK-N-SH neuroblastoma cells, SK-N-MC neuroepithelioma cells, and normal primary, BJ, and WI38 fibroblasts. Phase-contrast, fluorescence, and time-lapse video microscopy; flow cytometry; and Western blotting were used to investigate the effects of PV-10 on SK-N-AS and IMR5 cells. Synergy with commonly used anticancer drugs was determined by calculation of combination indices in SK-N-AS and IMR5 cells. Mouse xenograft models of SK-N-AS and IMR5 tumors were also used to evaluate the efficacy of PV-10 in vivo.
Results: In vitro preclinical data demonstrate that pharmacologically relevant concentrations of PV-10 are cytotoxic to neuroblastoma cell lines. Studies to investigate target modulation in neuroblastoma cell lines show that PV-10 disrupts lysosomes, decreases the percentage of cells in S phase, and induces apoptosis in a concentration-, time-, and cell-line-dependent manner, and we also identify agents that are synergistic with PV-10. Furthermore, experiments in xenograft mouse models show that PV-10 induces tumor regression in vivo.
Conclusion: Our study provides preclinical data on the efficacy of PV-10 against neuroblastoma and provides rationale for the development of an early phase clinical trial of this agent in relapsed and refractory neuroblastoma patients.

Keywords: neuroblastoma, PV-10, Rose Bengal, novel therapeutics, intralesional, oncolytic, immunotherapy

Introduction

Currently, children with relapsed or metastatic solid tumors such as Ewing sarcoma, neuroblastoma, osteosarcoma, and rhabdomyosarcoma have a low overall survival rate of <30%.[1] Of the pediatric solid tumors, neuroblastoma is the most common extracranial cancer in children and a leading cause of death in children aged 1–4 years.[2] It originates from sympathetic nervous tissue and is a very heterogeneous and complex disease.[3] Recent improvements in the treatment of neuroblastoma have increased 5-year survival rates for low-risk disease to over 90%.[4] However, >40% of patients presenting with neuroblastoma are considered high risk and despite introduction of intensive

Correspondence: Aru Narendran
POETIC Laboratory for Preclinical and Drug Discovery Studies, Division of Pediatric Oncology, Alberta Children's Hospital, University of Calgary, 2888 Shaganappi Trail NW, Calgary, AB, T3B 6A8, Canada
Tel +1 403 210 6418
Fax +1 403 955 2645
Email a.narendran@ucalgary.ca

submit your manuscript | www.dovepress.com
Dovepress
http://dx.doi.org/10.2147/OTT.S191478

treatment regimens, 5-year survival rates for these patients are below 50%.[2,4] In addition, the prognosis for relapsed neuroblastoma is dismal, with a 5-year survival rate of <10%.[4] Given the poor survival rates of neuroblastoma patients with refractory/relapsed disease, novel therapeutic approaches for the treatment of this disease are urgently needed.

PV-10 (Rose Bengal, 4,5,6,7-tetrachloro-2′,4′,5′,7′-tetraiodofluorescein disodium) has been previously used as a diagnostic agent to measure liver function in both adult and pediatric patients.[5,6] Previous studies have shown that PV-10 accumulates in lysosomes[7] and induces cell death in a range of adult cancers.[8–12] In a Phase II clinical trial for patients with refractory metastatic melanoma, intralesional injection of PV-10 induced tumor regression with an overall response rate of 51%.[13] PV-10 also demonstrated efficacy in combination with radiotherapy in a Phase II clinical trial for patients with in-transit or metastatic melanoma, with an overall response rate of 87%.[14] In addition to inducing direct cancer cell death, PV-10 has also been shown to induce a tumor specific immune response in both mouse studies[8,9,15,16] and clinical trials.[11,13,17–19] Recently, it has also been shown that combined treatment of melanoma bearing mice with PV-10 and antibodies to blockade the PD-1/PD-L1 pathway enhanced antitumor effect, compared to treatment with either PV-10 or antibodies to the PD-1/PD-L1 pathway alone.[16] The efficacy of PV-10 in preclinical studies and clinical trials against adult tumors provides the rationale for studying the role of PV-10 in pediatric cancers. The objective of this investigation was to assess the activity of PV-10 against neuroblastoma in the preclinical setting.

Materials and methods

Cell lines and tissue culture

Neuroblastoma cell lines SK-N-AS (ATCC CRL-2137), SK-N-BE(2) (ATCC CRL-2271), SK-N-MC (ATCC HTB-10), and SK-N-SH (ATCC-HTB-11) were purchased from American Type Culture Collection (ATCC, Manassas, VA, USA). Neuroblastoma cell lines IMR5, LAN1, and SHEP were a kind gift from Dr Herman Yeger (The Hospital for Sick Children, Toronto, ON, Canada). Normal fibroblastic cell lines BJ and WI38 were a kind gift from Dr Tara Beattie (Charbonneau Cancer Institute, University of Calgary, AB, Canada). The use of gifted cell lines was approved by the University of Calgary ethics committee. Neuroblastoma cell lines are described in Table 1 which was compiled by

Table 1 Main features and genetic abnormalities of the neuroblastoma cell lines used in this study

Cell line	Cell type	Age/sex	Genetic abnormalities
SK-N-AS	Neuroblastoma Bone marrow metastasis Poorly differentiated	6/F	FLT3 Het G739R;[20] IGF-I expression;[21] No/low MDR1 expression;[21] MYCT1 overexpression;[20] NRAS Het Q61K;[20] Rb Het L477P[20]
SK-N-BE(2)	Neuroblastoma Bone marrow metastasis Previously treated	2/M	Analysis of clone M17 in COSMIC:[20] AKT3 overexpression;[20] *MYCN* amplification;[20] NF1 deletion-frameshift N664fs*1;[20] p53 Hom C42F, C135F[20]
IMR5	Neuroblastoma Primary	1/M	AKT3 overexpression;[20] *ALK* copy number gain;[20] mTOR Hom F1888V;[20] *MYCN* amplification[20]
LAN1	Stage IV Neuroblastoma Bone marrow metastasis	2/M	Not available in COSMIC.[20] ALK F1174L;[22] *MYCN* amplification;[23] p53 nonsense mutation at cysteine 182, absence of protein expression[24]
SK-N-SH	Neuroblastoma Bone marrow metastasis	4/F	ALK Het F1174L, overexpressed;[20] MYCT1 overexpression[20]
SHEP	Neuroblastoma Lacks most neuronal characteristics Derived from SK-N-SH Previously treated	4/F	Not available in COSMIC:[20] Derived from SK-N-SH. 47,XX,der(1)inv dup(1)(q11q24) inv(1)(q25q44)dup91 (q25q44),+7,add(9)(q34),der(22)t(17;22)(q21;q13)[21]
SK-N-MC	Neuroepithelioma Metastatic	14/F	Normal chromosomes N3 and N10 are absent, and many (N1, N2, N4, N15, N16, N17, N21, and N22) are monosomic. Normal chromosome N8 is most often tetrasomic. The remainder of normal chromosomes were usually paired. Numerous marker chromosomes are present including: 1p+, der(3)t(2;3)(q24;q27), del(4)(p12), 11q+, del(2)(q23), ampl.(17)(p12), ampl.(16)(q13), del(15)(q13q22), 21p+, iso(3q), del(22)(q11q13)[21] Analysis of clone MC-IXC in COSMIC:[20] *MYC* copy number gain;[20] *PTEN* copy number loss;[20] Rb Hom R698M/S (2 different substitutions at same codon);[20] p53 Het c.1_169del395[20]

Abbreviations: add, addition; ampl, amplification; COSMIC, catalog of somatic mutations in cancer; del, deletion; der, derivative; dup, duplication; F, female; Het, heterozygous; Hom, homozygous; ins, insertion; inv, inversion; iso, isoform; M, male.

searching the Catalog of Somatic Mutations In Cancer (COSMIC) cell lines database[20] and a review of the literature.[21–24] All cell lines were cultured in DMEM (Thermo Fisher Scientific, Waltham, MA, USA) supplemented with 5% (v/v) heat-inactivated FBS (Thermo Fisher Scientific), 100 units/mL penicillin, and 100 units/mL streptomycin (Thermo Fisher Scientific). Cell cultures were maintained at 37°C in a humidified incubator with 5% CO_2, protected from exposure to light. Lymphocytes were isolated from the bone marrow sample by density gradient centrifugation using Ficoll-Paque Plus (GE Healthcare Life Sciences, Mississauga, ON, Canada), as described previously.[25]

The primary bone marrow sample was approved by the local Research Ethics Board (Ethics ID #17184) and written informed consent was obtained. All applicable international, national, and institutional guidelines for the care and use of animals were followed. All animal procedures were carried out in accordance with the guidelines of the Canadian Council on Animal Care and the NIH guidelines on the care and use of laboratory animals. All protocols were reviewed and approved by the Animal Care Committee of the University of Calgary (Protocol approval number: AC16-0243).

Materials and reagents

PV-10 (10% solution of Rose Bengal disodium in 0.9% saline) was provided by Provectus Biopharmaceuticals Inc. (Knoxville, TN, USA) and stored and protected from light at room temperature. Stock solutions of doxorubicin, etoposide, vincristine, cisplatin, pegaspargase, irinotecan, and cytarabine were obtained from the Alberta Children's Hospital Pharmacy (Calgary, AB, Canada) and stored at room temperature and protected from exposure to light. For subsequent experiments, the drugs were diluted in DMEM plus supplements to the appropriate concentrations.

Cytotoxicity assays

Cells were seeded in 96-well plates (Greiner BioOne, Monroe, NC, USA) at 5×10^3 per well in 100 µL DMEM and cultured for 24 hours. PV-10 alone or PBS (137 mM NaCl, 2.7 mM KCl, 10 mM Na_2HPO_4, 1.8 mM KH_2PO_4, pH 7.25) (vehicle control) was diluted in DMEM and 100 µL was added to each well. All treatments were run in triplicate at final concentrations ranging from 3.125 to 400 µM. Plates were cultured for 96 hours, protected from light. Wells were washed twice with PBS, 200 µL fresh DMEM was added to each well and cell viability was evaluated using the alamar blue (Thermo Fisher Scientific) cytotoxicity assay as per manufacturer's instructions. Half maximal inhibitory concentrations (IC_{50}) were determined using CompuSyn software (ComboSyn Inc., Paramus, NJ, USA).

Light microscopy

Cells were seeded in six-well plates (Corning Incorporated, Corning, NY, USA) at 2×10^5 per well and cultured for 24 hours. The cells were treated with either PBS (vehicle control) or PV-10 and cultured for 96 hours, protected from light. At 24 and 96 hours posttreatment, phase-contrast images were captured on a Zeiss Axiovert 200M microscope with a Zeiss AxioCam MRm Rev.3 FireWire camera using Zeiss AxioVision Se64 software. Images were processed using Adobe Photoshop (Adobe Creative Cloud 2017).

Time-lapse video microscopy

Cells were seeded in 96-well plates (Greiner BioOne) at 5×10^3 cells per well and cultured for 24 hours. The cells were treated with either PBS (vehicle control) or PV-10. Three images per well were captured every 30 minutes for 48 hours using an IncuCyte Zoom microscope and IncuCyte Zoom software (Essen BioScience, Ann Arbor, MI, USA) located in a humidified incubator with 5% CO_2 at 37°C. Cell number in each well was counted using ImageJ software and normalized to cell number at 0 h. At least 350 cells were counted per treatment per experiment.

Lysosome detection and fluorescence microscopy

Cells were seeded onto sterile coverslips in six-well plates (Corning Incorporated) at 2×10^5 per well for untreated cells and 6×10^5 per well for treated cells and cultured for 24 hours. The cells were treated with either PBS (vehicle control) or PV-10 for 6 hours, protected from light. Wells were washed twice with PBS and 2 mL DMEM containing 2.5 µg/mL Hoechst 33342 stain (Thermo Fisher Scientific) was added to each well. The cells were incubated protected from light at 37°C for 10 minutes and then Lysotracker Green DND-26 (Thermo Fisher Scientific) was added to the media at 500 nM final concentration. Then the cells were cells were incubated protected from light at 37°C for 15 minutes, coverslips were mounted onto glass slides at time of imaging, and images were captured on a Zeiss Axiovert 200M microscope with a Zeiss AxioCam MRm Rev.3 FireWire camera using Zeiss AxioVision Se64 software. Images were processed using Adobe Photoshop (Adobe Creative Cloud 2018).

Flow cytometry

To analyze cell cycle alterations, the cells were seeded in 100 mm dishes (Corning Incorporated), so that a minimum

of 2×10^6 cells could be collected posttreatment. The cells were cultured for 24 hours, treated with either PBS (vehicle control) or PV-10 and cultured for either 16 or 24 hours, protected from light. Then they were collected by trypsinization, washed with PBS, filtered through a 40 μm nylon cell strainer (Falcon, Corning, NY, USA), counted by trypan blue staining using a hemocytometer, re-suspended in 0.9% (w/v) sterile NaCl, and fixed in ice-cold 90% (v/v) ethanol. Samples were incubated at room temperature for 30 minutes then stored at −20°C. For analysis, samples were centrifuged at 1,400 rpm for 5 minutes at 4°C and washed twice with ice-cold PBS. The cells were then incubated at 37°C for 20 minutes in 300 μL labeling buffer: 10 μg/mL DAPI (Sigma-Aldrich Co., St Louis, MO, USA), 200 μg/mL RNase A (Sigma-Aldrich Co.) in 0.1% Triton X-100 in PBS. The samples were run on a BD Bioscience LSR II cytometer using Diva 6.1.3 software (BD Bioscience, Mississauga, ON, Canada). The results were analyzed using ModFitLT 3.3 software (Verity Software House, Topsham, ME, USA).

Preparation of cellular extracts for Western blotting

Cells were seeded at 1×10^6 in 100 mm dishes (Corning Incorporated) and cultured for 24 hours. The cells were then treated with either PBS (vehicle control) or PV-10 and cultured for 24 hours, protected from light. Media were collected from cell cultures, and the cells were washed with PBS and collected following trypsinization. The cells were then washed in ice-cold PBS and centrifuged at 1,200 rpm at 4°C for 5 minutes. The supernatant was removed, and the pellet was resuspended in RIPA buffer (50 mM Tris-HCl (pH 8), 150 mM NaCl, 1% (v/v) NP-40, 0.5% (w/v) sodium deoxycholate, 0.1% (w/v) sodium dodecyl sulfate [SDS]) supplemented with 1% (v/v) phosphatase inhibitor (Sigma-Aldrich Co.) and 1% (v/v) protease inhibitor (Sigma-Aldrich Co.). The samples were transferred to 1.5 mL tubes, incubated on ice for 10 minutes, vortexed and centrifuged at 12,000 rpm for 10 minutes. The supernatants were collected as whole cell lysates and either used immediately or stored at −20°C.

Western blotting

Western blotting was performed as described previously.[25] Briefly, proteins were transferred to nitrocellulose membrane using a Trans-Blot Turbo Transfer System (BioRad, Montreal, QC, Canada), transfer was confirmed using Ponceau S stain (0.1% (w/v) in 5% (v/v) acetic acid) and the membranes were blocked in 5% skim milk in Tris-buffered saline with 0.1% (v/v) Tween-20 (TBS-T; 50 mM Tris-HCl, pH 7.5, 150 mM NaCl, 0.1% (v/v) Tween-20) at room temperature for 2 hours. The membranes were incubated overnight at 4°C with the following primary antibodies diluted in 5% (w/v) skim milk in TBS-T: anti-poly-(ADP-ribose) polymerase (PARP) (1:3,000, 9542S; Cell Signaling Technology, Whitby, ON, Canada), anti-caspase 3 (1:500, 9662S; Cell Signaling Technology), anti-caspase 7 (1:1,000, 9492S; Cell Signaling Technology), anti-caspase 9 (1:1,000, 9502S; Cell Signaling Technology), and anti-β-actin (1:5,000, 8457L; Cell Signaling Technology). Membranes were washed three times with TBS-T, incubated with anti-rabbit secondary antibody (1:3,000, 7074S, Cell Signaling Technology), washed three times with TBS-T, incubated with Western Lightning Plus-ECL reagent (PerkinElmer Inc., Waltham, MA, USA) for 2 minutes, and developed using the chemiluminescence setting on a ChemiDoc MP Imaging System (BioRad).

Combination screens

The cells were cultured as described for cytotoxicity assays. Test drugs (doxorubicin, etoposide, vincristine, cisplatin, pegaspargase, irinotecan, and cytarabine) were prepared at a final concentration of 0.1 μM in media containing either PBS (vehicle control) or PV-10 (50 μM final). Treatments were added to cells in triplicate. Plates were cultured and washed, and cell viability was analyzed by alamar blue, as described for cytotoxicity assays.

Combination studies

The cells were cultured as described for cytotoxicity assays. Dilution series of test drugs (doxorubicin, etoposide, and vincristine) were prepared in DMEM containing either PBS (vehicle control) or PV-10 (50 μM final) and added to cells in triplicate. Plates were cultured and washed, and cell viability was analyzed by alamar blue, as described for cytotoxicity assays. Combination indices (CIs) for IC_{50} of test drug in combination with 50 μM PV-10 were calculated using CompuSyn software (ComboSyn Inc, Paramus, NJ, USA). CI values were scored according to the following criteria $CI < 1$ indicated synergistic activity, $CI = 1$ indicated additive activity, and $CI > 1$ indicated antagonistic activity.[26]

Radiosensitivity assays

Cells were seeded at 5×10^4 in 60 mm dishes (Corning Incorporated) and incubated for 24 hours. The cells were then treated with either PBS (vehicle control) or 50 μM PV-10 and cultured for 4 hours, protected from light. Cells were irradiated with 0.5, 1, or 2 Gray (Gy) using a Gammacell

1,000 Elite (MDS Nordion, Kanata, ON, Canada) and cultured for 92 hours in the dark. Treatments were run in triplicate. Dishes were washed twice with PBS and cell viability was analyzed by alamar blue, as described for cytotoxicity assays.

In vivo xenograft models

All animal procedures were carried out in accordance with the guidelines of the Canadian Council on Animal Care and the NIH guidelines on the care and use of laboratory animals. All protocols were reviewed and approved by the Animal Care Committee of the University of Calgary (Protocol approval number: AC16-0243).

IMR5-mCherryFluc and SK-N-AS-mCherryFluc cells were used in the animal studies. These cell lines stably expressed enhanced firefly luciferase and mCherry on a self-inactivating lentiviral vector encoding the internal U3 region from murine stem cell virus (mscv), enhanced firefly luciferase (effLuc), the internal ribosomal entry site (IRES) element from encephalomyocarditis virus (emcv), and mCherry.

Six- to eight-week-old female CB17 severe combined immunodeficiency (SCID) mice (Charles River Laboratories, Saint-Constant, QC, Canada) were subcutaneously injected in the right flank with 2.5×10^6 cells (SK-N-ASmCherryFluc or IMR5mCherryFluc) suspended in 0.1 mL Matrigel Matrix (Thermo Fisher Scientific) (day 0). After tumor injection, animals with detectable tumor growth of at least 25 mm^2 were randomized into treatment groups. The groups were treated with either 50 µL PBS (vehicle control) or 50 µL PV-10 or 25 µL PV-10 by intralesional injection, according to a previously established protocol.[9] Animals were monitored daily and tumor areas were determined with a Vernier caliper. When tumors reached the defined end point of 225 mm^2, mice were euthanized. Animals that remained tumor free were kept for 120 days posttreatment. Tumor growth was also monitored using the Xenogen IVIS 200 system (Xenogen Corporation, Alameda, CA, USA). Mice were imaged to document bioluminescent signal emitted from tumors, following intraperitoneal injection of D-Luciferin (Gold Biotechnology, Olivette, MO, USA). Data were analyzed by determining total photon flux emission (photons/s) in the region of interest, as per established methods.[27]

Statistical analysis

Data were analyzed from three independent experiments, unless stated otherwise in the figure legends. Data were plotted as mean ± standard errors of the mean. Data were analyzed using GraphPad Prism 7 (GraphPad Software, Inc., La Jolla, CA, USA). Values were considered significantly different when $P<0.05$.

Results

PV-10 inhibits growth of neuroblastoma cell lines

To determine the effects of PV-10 on neuroblastoma, we treated neuroblastoma (Figure 1A) (described in Table 1) and normal fibroblast (Figure 1B) cell lines and a normal primary bone marrow sample (Figure 1B) with a range of concentrations of PV-10 (3.125–400 µM) for 96 hours and cell viability was measured using alamar blue. PV-10 decreased cell viability in a concentration-dependent manner in all cell lines tested. We calculated IC_{50} values for the neuroblastoma cell lines (Table 2), and the values ranged from 49 to 85 µM, with a mean of 71 µM (Figure 1C). By contrast, IC_{50} values for the normal fibroblast cell lines and primary bone marrow sample (Table 3) were higher and ranged from 93 to 143 µM, with a mean of 124 µM (Figure 1C).

PV-10 is cytotoxic to neuroblastoma cell lines

We next investigated whether PV-10 was cytotoxic or cytostatic to neuroblastoma cell lines. We chose to study two different cell lines (SK-N-AS and IMR5), which had different sensitivities to PV-10, based on IC_{50} values, and different gene mutations and copy number variation. Cells were treated with either PBS (vehicle control) or 50, 100, or 150 µM PV-10 for 96 hours and observed at 24 and 96 hours posttreatment by phase-contrast light microscopy (Figure 2A). By 96 hours, SK-N-AS and IMR5 cells treated with PBS grew to confluency. SK-N-AS and IMR5 cells treated with 50 µM PV-10 did not grow to confluency by 96 hours, but few dead cells were observed. By contrast, dead IMR5 cells were visible 24 hours posttreatment with 100 and 150 µM PV-10 and by 96 hours few of these treated IMR5 cells remained attached to the plate. SK-N-AS cells appeared to be less sensitive to PV-10, compared to IMR5 cells. At 24 hours posttreatment with 100 µM PV-10, few dead SK-N-AS cells were observed. By 96 hours, 100 and 150 µM PV-10 were cytotoxic to SK-N-AS cells; however, more cells remained attached to the plate following treatment with 100 µM PV-10, compared to IMR5 cells.

Neuroblastoma cell lines display different sensitivities to PV-10

To investigate the different sensitivities of the two cell lines (SK-N-AS and IMR5) to PV-10, we used time-lapse video

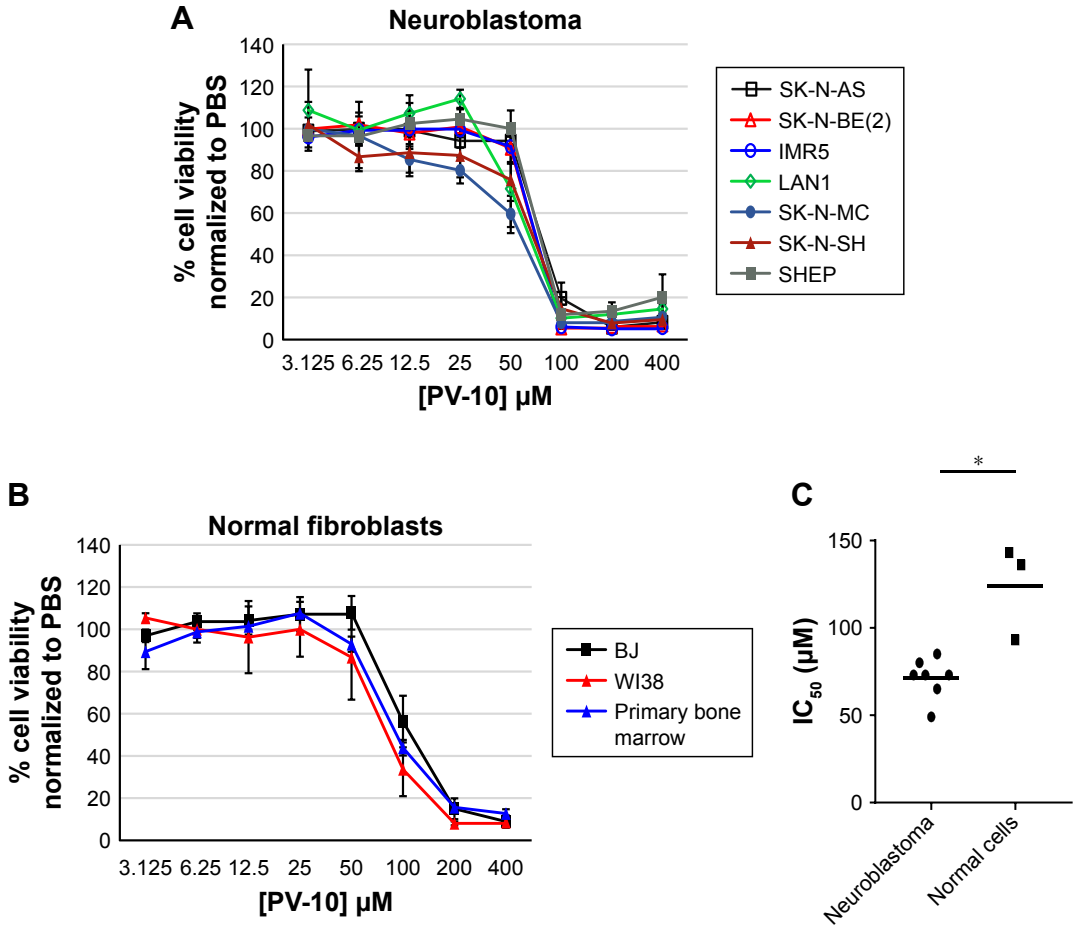

Figure 1 PV-10 decreases cell viability in neuroblastoma cell lines.
Notes: (**A**) Different neuroblastoma cell lines were treated with increasing concentrations (3.125–400 µM) of PV-10 for 96 hours. Cell viability was measured by alamar blue assay. Percent cell viability was normalized to corresponding treatment with PBS (vehicle control). Mean percentages of cell viability calculated from three separate experiments and standard errors of the means are shown. (**B**) Different normal fibroblastic cell lines and a primary bone marrow sample were treated with increasing concentrations (3.125–400 µM) of PV-10 for 96 hours. Cell viability was measured by alamar blue assay. Percent cell viability was normalized to corresponding treatment with PBS (vehicle control). Mean percentages of cell viability calculated from three separate experiments and standard errors of the means are shown. (**C**) The mean and distribution of PV-10 IC_{50} values (µM) for cell lines from Figure 1A+B. Asterisk shows significant difference, unpaired Student's *t*-test, $P<0.05$.
Abbreviation: IC_{50}, half maximal inhibitory concentration.

microscopy to quantify the percentage of cells attached to the plate following 12, 24, 36, and 48 hours treatment with 100 µM PV-10. Number of cells attached posttreatment was normalized to cell number at 0 hours (Figure 2B). SK-N-AS cells were less sensitive to treatment than IMR5 cells. At 12 hours 89%, and at 48 hours 41%, of SK-N-AS cells were attached to the plate. By comparison, at 12 hours 16%, and at 48 hours 2%, of IMR5 cells were attached to the plate. These data show that IMR5 cells are more sensitive to treatment than SK-N-AS cells.

Table 2 Half maximal inhibitory concentration (IC_{50}) values for PV-10-treated neuroblastoma cell lines 96 hours posttreatment

Cell line	Cell type	PV-10 IC_{50}, (µM)	SD
SK-N-AS	Neuroblastoma	85	6
LAN1	Neuroblastoma	80	5
SK-N-BE(2)	Neuroblastoma	73	3
IMR5	Neuroblastoma	73	10
SHEP	Neuroblastoma	73	8
SK-N-SH	Neuroblastoma	65	10
SK-N-MC	Neuroepithelioma	49	10

Table 3 Half maximal inhibitory concentration (IC_{50}) values for PV-10-treated normal fibroblast cell lines and a primary bone marrow sample 96 hours posttreatment

Cell line	Cell type	PV-10 IC_{50}, (µM)	SD
BJ	Normal fibroblast (foreskin)	143	10
Primary bone marrow	Normal primary fibroblasts	136	10
WI38	Normal fibroblast (lung)	93	8

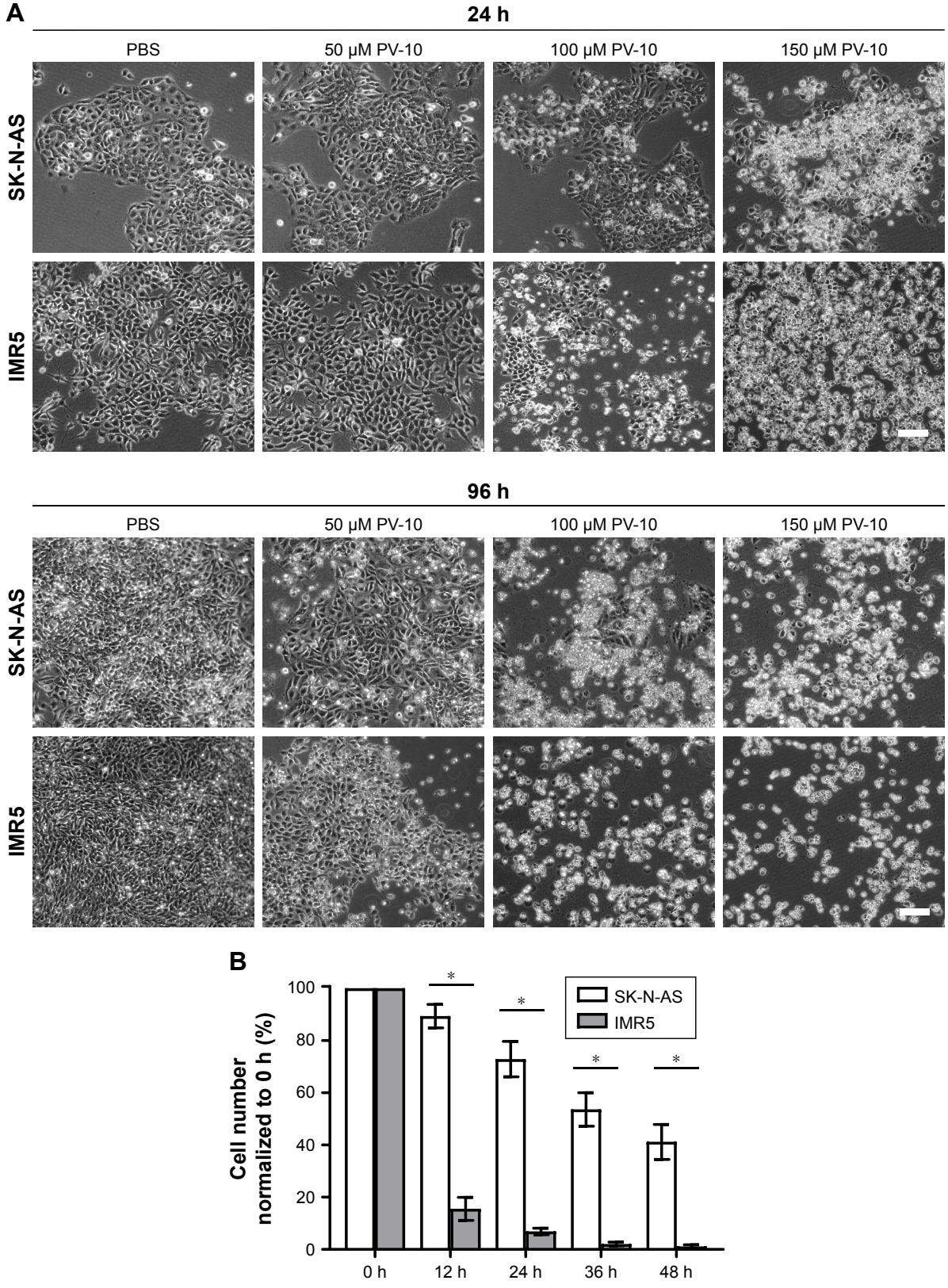

Figure 2 PV-10 is cytotoxic to neuroblastoma cell lines.

Notes: (**A**) Neuroblastoma cell lines SK-N-AS and IMR5 were treated with either PBS (vehicle control) or 50 or 100 μM PV-10 for 24 and 96 hours and observed by phase-contrast light microscopy. Experiments were performed three times and representative images are shown. Scale bars = 100 μm. (**B**) Neuroblastoma cell lines SK-N-AS and IMR5 were treated with either PBS (vehicle control) or 100 μM PV-10 and observed by time-lapse video microscopy. Images were captured every 30 minutes for 48 hours. Cell number was counted and normalized to cell number at 0 hours. At least 350 cells were counted per treatment per experiment. Mean percentages of cell number calculated from three separate experiments and standard errors of the means are shown. Asterisks show significant differences, unpaired Student's *t*-test, $P<0.05$.

Treatment with PV-10 disrupts lysosomes

Previously, PV-10 has been shown to induce loss of lysosome integrity.[7] We therefore treated SK-N-AS and IMR5 cells with either PBS (vehicle control) or 100 µM PV-10 for 6 hours, stained live cells with the nucleic acid stain Hoechst 33342 and LysoTracker Green DND-26 (which concentrates and fluoresces in acidic organelles) and observed cells by fluorescence microscopy (Figure 3A). In PBS-treated SK-N-AS and IMR5 cells and in SK-N-AS PV-10-treated cells, lysosomes were visible as specific foci. By contrast, lysosomal foci were no longer visible in PV-10-treated IMR5 cells. As SK-N-AS cells were less sensitive to PV-10 than IMR5 cells, we next observed lysosomes in SK-N-AS cells treated for 6 hours with an increased concentration of PV-10 (200 µM) (Figure 3B). As observed in IMR5 cells treated with 100 µM PV-10, lysosomal foci were not visible in 200 µM PV-10 SK-N-AS cells, indicating that PV-10 disrupts lysosomes in both the cell lines tested.

PV-10 treatment decreases the percentage of cells in S phase of the cell cycle

Next, to further determine target modulation of PV-10, we analyzed the effect of PV-10 upon the cell cycle. SK-N-AS and IMR5 cells were treated with either PBS (vehicle control) or 50 or 100 µM PV-10 for 6, 16, or 24 hours. Cells were then fixed in ethanol, stained with DAPI, and analyzed by flow cytometry. Treatment of IMR5 cells with 100 µM PV-10 decreased the percentage of cells in S phase and increased the percentage of cells in G1 phase, in a time-dependent manner (Figure 4A). At 6 hours, no changes in cell cycle

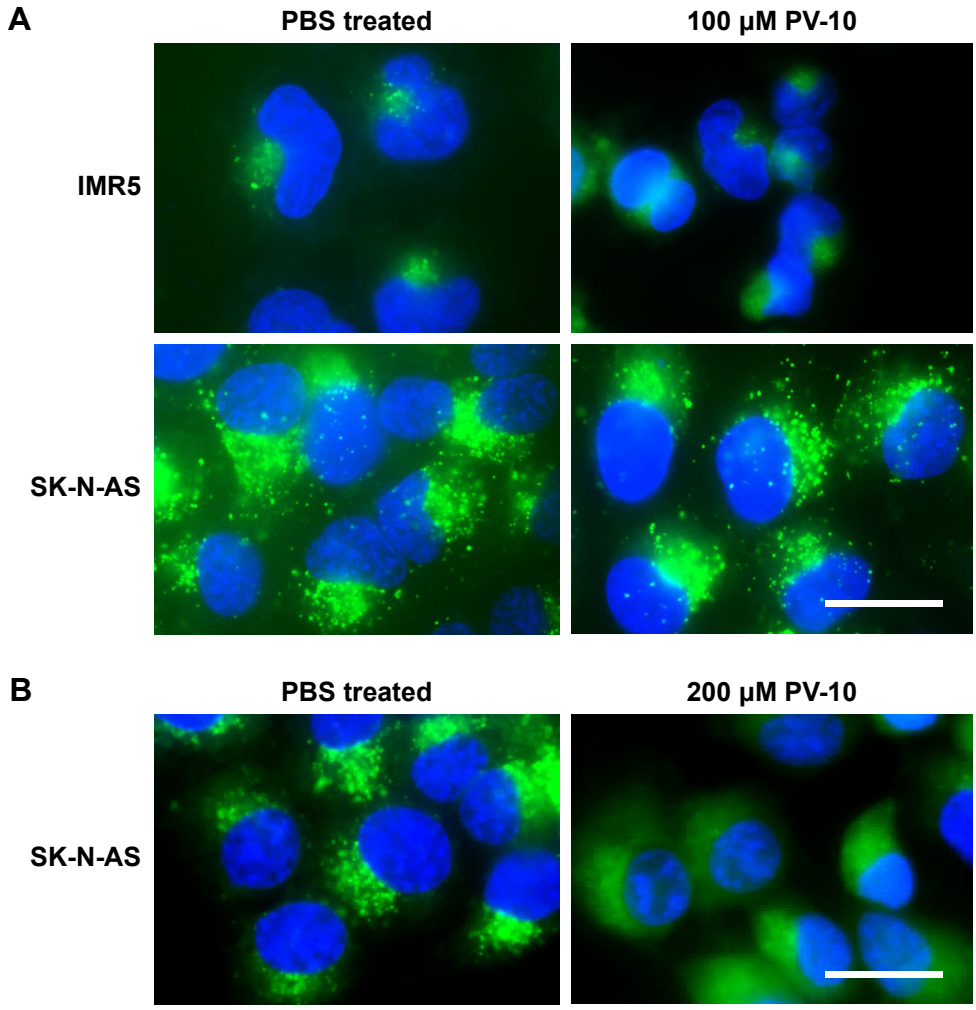

Figure 3 PV-10 disrupts lysosomes.
Notes: Live cells were stained with the nucleic acid stain Hoechst 33342 and LysoTracker green DND-26, which concentrates and fluoresces in acidic organelles, and observed by fluorescence microscopy. (**A**) Neuroblastoma cell lines IMR5 and SK-N-AS were treated with either PBS (vehicle control) or 100 µM PV-10 for 6 hours. (**B**) Neuroblastoma cell line SK-N-AS was treated with either PBS (vehicle control) or 200 µM PV-10 for 6 hours. Scale bars = 20 µm. Data presented are representative of three separate experiments.

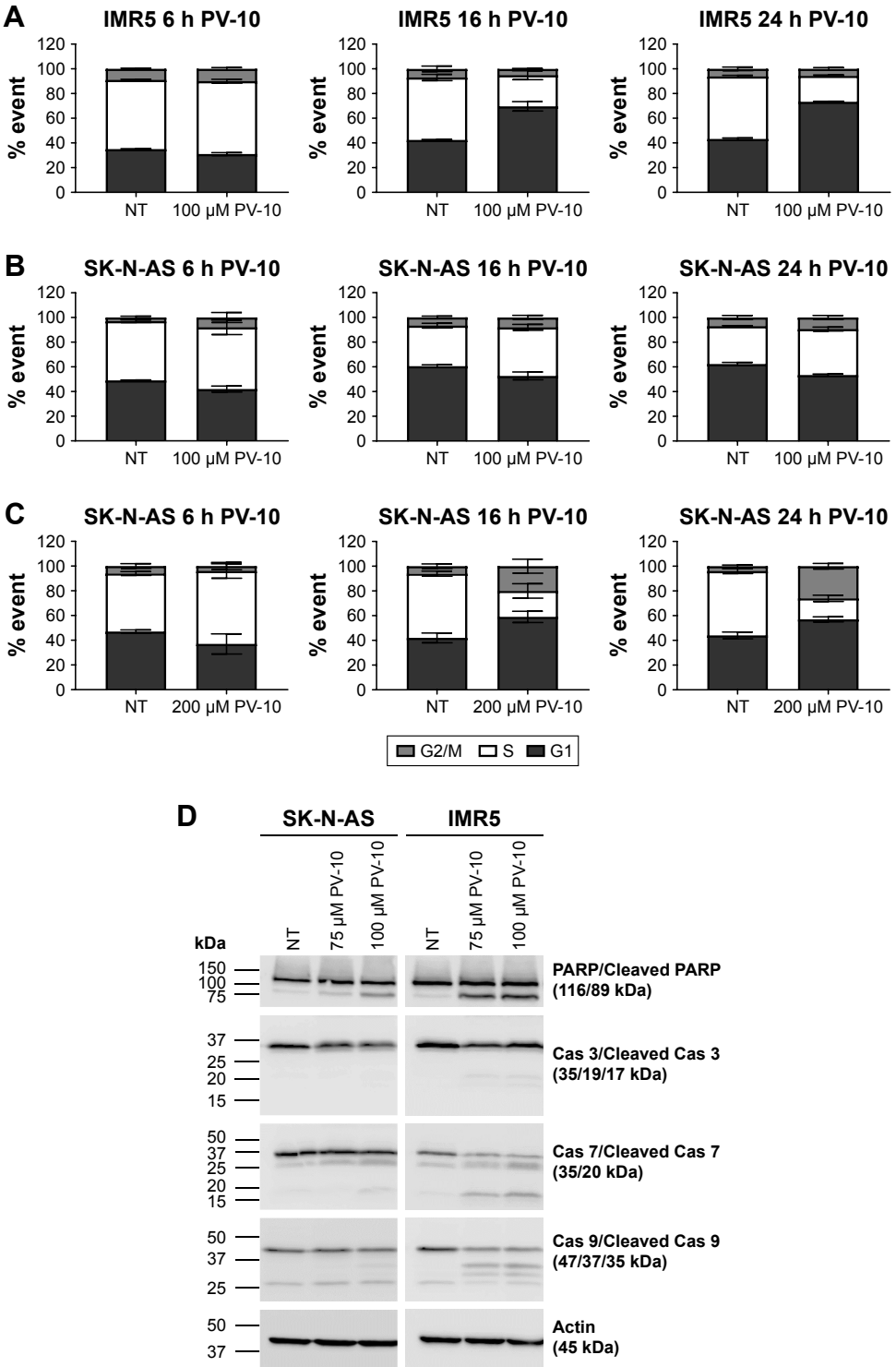

Figure 4 PV-10 decreases the percentage of cells in S phase of the cell cycle and induces cell death by apoptosis.

Notes: (**A**) Neuroblastoma cell line IMR5 was treated with either PBS (vehicle control) or 100 μM PV-10 for 6, 16, or 24 hours, fixed in ethanol, stained with DAPI, and analyzed by flow cytometry to detect cell cycle phase. Mean percentages of cells in G1, S, or G2/M phase of the cell cycle were calculated from three separate experiments and standard errors of the means are shown. (**B**) Neuroblastoma cell line SK-N-AS was treated with either PBS (vehicle control) or 100 μM PV-10 for 6, 16, or 24 hours, fixed in ethanol, stained with DAPI, and analyzed by flow cytometry to detect cell cycle phase. Mean percentages of cells in G1, S, or G2/M phases of the cell cycle were calculated from three separate experiments and standard errors of the means are shown. (**C**) Neuroblastoma cell line SK-N-AS was treated with either PBS (vehicle control) or 200 μM PV-10 for 6, 16 or 24 hours, fixed in ethanol, stained with DAPI, and analyzed by flow cytometry to detect cell cycle phase. Mean percentages of cells in G1, S, or G2/M phase of the cell cycle were calculated from three separate experiments and standard errors of the mean are shown. (**D**) Neuroblastoma cell lines SK-N-AS and IMR5 were treated with either PBS (vehicle control) or 75 or 100 μM PV-10 for 24 hours. Total cell lysates were prepared and analyzed by Western blotting to detect the levels of total and cleaved PARP, caspase 3, caspase 7, and caspase 9. Actin was used as a loading control. Molecular masses are indicated in kilodaltons. Data presented are representative of three separate experiments.

distribution between treated and untreated IMR5 cells were observed. However, at 16 hours, there was a 27% increase in G1 phase cells and a 25% decrease in S phase cells, when compared to untreated cells. Similarly, at 24 hours, there was a 30% increase in G1 phase cells and a 30% decrease in S phase cells, posttreatment with 100 μM PV-10. Treatment of SK-N-AS cells with 100 μM PV-10 did not affect the cell cycle at the times tested (Figure 4B). We therefore analyzed the cell cycle distribution of SK-N-AS cells treated with an increased concentration of 200 μM PV-10. Treatment of SK-N-AS cells with 200 μM PV-10 decreased the percentage of cells in S phase and increased the percentages of cells in G1 and G2/M phases of the cell cycle, in a time-dependent manner (Figure 4C). At 6 hours, no changes in cell cycle distribution between treated and untreated SK-N-AS cells were observed. However, at 16 hours, there was a 31% decrease in S phase cells corresponding to a 17% increase in G1 phase cells and a 14% increase in G2/M phase cells. Likewise, at 24 hours, there was a 35% decrease in S phase cells corresponding to a 13% increase in G1 phase cells and a 22% increase in G2/M phase cells. These results show that treatment with PV-10 leads to a time-dependent increase in G1 phase cells and decrease in S phase cells, in both the cell lines. In addition, PV-10 has cell line-specific effects on the cell cycle, as the treatment increased the percentage of G2/M cells in SK-N-AS but not IMR5 cells.

Treatment with PV-10 induces cancer cell apoptosis

Analysis by Western blotting was then performed to investigate if PV-10-treated cells were undergoing apoptosis. SK-N-AS and IMR5 cells were treated with either PBS (vehicle control) or 75 or 100 μM PV-10 for 24 hours. Total cell extracts were analyzed by Western blotting to detect the levels of total and cleaved poly (ADP-ribose) polymerase (PARP), total and cleaved caspase 3, total and cleaved caspase 7, total and cleaved caspase 9 and actin (loading control) (Figure 4D).

PV-10 treatment showed concentration-dependent cleavage of PARP. Treatment with 100 μM PV-10 induced PARP cleavage in both of the cell lines. SK-N-AS cells treated with 75 μM PV-10 showed less PARP cleavage than cells treated with 100 μM PV-10, whereas IMR5 cells had similar levels of PARP cleavage when treated with 75 and 100 μM PV-10. Activation of caspases 3, 7, and 9 was dependent on PV-10 concentration and the cell line. Cleaved caspase 3 was present in IMR5 cells treated with 100 μM PV-10. Levels of total caspase 7 were lower in IMR5 cells treated with both 75 and 100 μM PV-10 compared to untreated cells and cleaved caspase 7 was detected in SK-N-AS cells treated with 100 μM PV-10 and in IMR5 cells treated with 75 and 100 μM PV-10. Levels of total caspase 9 were lower in 75 and 100 μM PV-10-treated IMR5 cells than in untreated cells and cleaved caspase 9 was also detected in these samples. These data indicated that the cell death induced by PV-10 was via apoptosis.

PV-10 is synergistic with different anticancer agents

To investigate which commonly used anticancer drugs could be combined with PV-10 to enhance cytotoxicity, we first screened SK-N-AS and IMR5 cells against a panel of seven conventional chemotherapeutic agents, with different mechanisms of action (Figure 5). All the agents were screened at 0.1 μM, alone and in combination with the sub-cytotoxic concentration of 50 μM PV-10, and cell viability was determined using the alamar blue assay, 96 hours posttreatment. Based on these results, the agents that showed the largest increase in cytotoxicity when combined were selected for further study to determine CIs and synergy. Agents evaluated for CI studies were doxorubicin, etoposide, and vincristine. SK-N-AS and IMR5 cells were treated with doxorubicin, etoposide, or vincristine alone or in combination with 50 μM PV-10, and cell viability was determined using the alamar blue assay, 96 hours posttreatment. All the agents demonstrated synergism with 50 μM PV-10 (Table 4).

PV-10 induces radiosensitivity in neuroblastoma cell lines

In addition to conventional chemotherapeutic agents, we investigated if PV-10 enhanced the effect of treatment with ionizing radiation (IR) in SK-N-AS (Figure 6A) and IMR5 (Figure 6B) cells. Cells were pretreated for 4 hours with either PBS (vehicle control) or 50 μM PV-10 and then irradiated with 0.5, 1, or 2 Gy. Cell viability was measured by alamar blue 96 hours after initial treatment. Pretreatment with 50 μM PV-10 enhanced the effect of IR in both SK-N-AS and IMR5 cells. For SK-N-AS cells, cell viability decreased by 54.8%, 58.7%, and 60% when cells were pretreated with PV-10 for 4 hours prior to irradiation with 0.5, 1, or 2 Gy, respectively, compared to irradiation alone. For IMR5 cells, cell viability decreased by 24%, 21%, and 13% when cells were pretreated with PV-10 for 4 hours prior to irradiation with 0.5, 1, or 2 Gy, respectively, compared to irradiation alone.

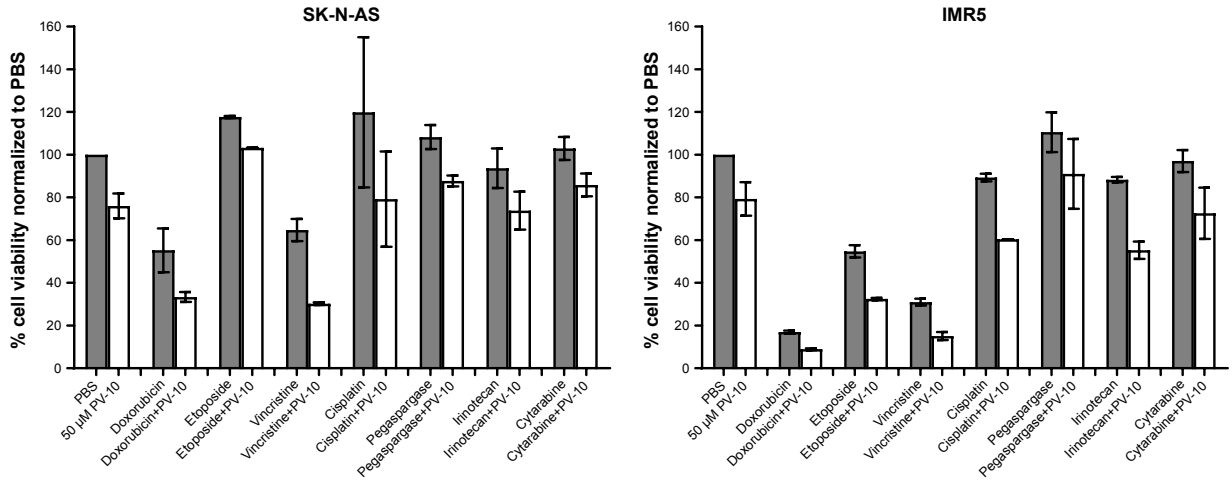

Figure 5 PV-10 is synergistic with different anticancer agents.
Notes: Neuroblastoma cell lines SK-N-AS and IMR5 were treated with 0.1 μM of seven different anticancer agents either alone or in combination with 50 μM PV-10. Cells were treated for 96 hours and cell viability was measured by alamar blue. Percent cell viability was normalized to treatment with PBS (vehicle control). Mean percentages of cell viability calculated from two separate experiments and standard errors of the means are shown.

PV-10 treatment leads to tumor regression in vivo

To determine if PV-10 is also active in vivo, we characterized the effect of PV-10 intralesional injection on subcutaneous SK-N-AS and IMR5 tumors in CB17 SCID mice. Tumors were injected once with either 25 or 50 μL PV-10[9] and monitored daily. IMR5 tumors were very sensitive to treatment with PV-10 (Figure 7A and B). For control tumors, tumor size increased from 25.6 mm^2 6 days posttreatment to 172.9 mm^2 23 days posttreatment. By comparison, size of tumors treated with 25 μL PV-10 increased from 26.6 mm^2 to 41.2 mm^2 and size of tumors treated with 50 μL PV-10 increased from 27.9 mm^2 to 47.3 mm^2. Tumor growth was also quantified using a Xenogen IVIS 200 system which measured bioluminescent signal emitted from tumors, following intraperitoneal injection of D-Luciferin. Tumor size decreased following treatment with 25 and 50 μL PV-10 and remained low 17 days posttreatment. Treatment with PV-10 also increased survival, in a dose-dependent manner (Figure 7C). Control-treated mice had a median survival of 25.5 days, whereas 25 μL PV-10-treated mice survived a median of 41.5 days and 50 μL PV-10-treated mice survived a median of 76 days. Additionally, two of the mice treated with 50 μL PV-10 underwent complete tumor regression and remained tumor free for 120 days after treatment.

SK-N-AS tumors also responded to treatment with PV-10 (Figure 7D and E). For control tumors, tumor size increased from 28.9 mm^2 6 days posttreatment to 179.3 mm^2 18 days posttreatment. By comparison, size of tumors treated with 25 μL PV-10 increased from 25.3 to 92.1 mm^2 and size of tumors treated with 50 μL PV-10 increased from 29.3 to 57.5 mm^2. When measured using the Xenogen IVIS 200 system, tumor size decreased following treatment with 25 and 50 μL PV-10 and remained lower than control-treated tumors 15 days posttreatment. Treatment with PV-10 also increased survival (Figure 7F). Control-treated mice had a median survival of 29 days, whereas 25 μL PV-10-treated mice survived a median of 37 days and 50 μL PV-10-treated mice survived a median of 36 days. In addition, one mouse treated with 50 μL PV-10 underwent complete tumor regression and remained tumor free for 120 days following treatment.

Table 4 Combination indices for SK-N-AS and IMR5 neuroblastoma cell lines treated with doxorubicin, etoposide, or vincristine either alone or in combination with 50 μM PV-10 for 96 hours

Cell line	Doxorubicin	Etoposide	Vincristine
SK-N-AS	0.77	0.17	0.35
IMR5	0.38	0.65	0.2

Discussion

The overall survival rate for children with pediatric solid tumors is lower than that for children with hematological malignancies.[1] The most common extracranial pediatric solid tumor is neuroblastoma, which is a leading cause of death in children aged 1–4 years.[2] Given the poor survival rates of patients with neuroblastoma, and the morbidities associated with the intensive treatment regimens administered to

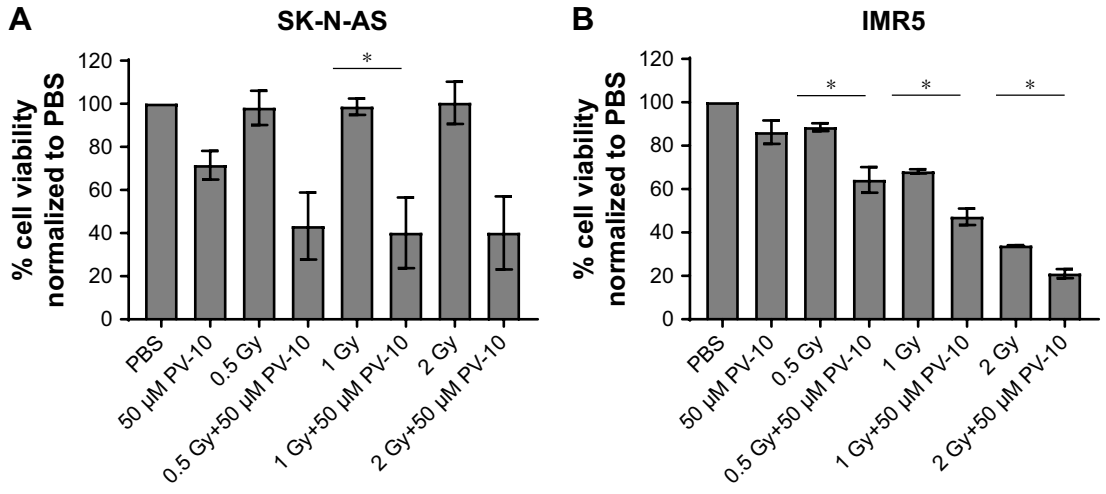

Figure 6 PV-10 enhances the effect of irradiation.

Notes: Neuroblastoma cell lines SK-N-AS (**A**) and IMR5 (**B**) were pretreated with either PBS (vehicle control) or 50 μM PV-10 for 4 hours. Cells were then irradiated with 0.5, 1, or 2 Gy and cultured for a further 92 hours. Cell viability was measured by alamar blue assay. Mean percentages of cell viability calculated from three separate experiments and standard errors of the means are shown. Asterisks show significant differences, paired Student's *t*-test, $P<0.05$.

high-risk and relapsed patients, there is an urgent unmet need to develop novel therapeutic approaches and early phase clinical trials for neuroblastoma patients.

PV-10 has been shown to demonstrate cytotoxicity and antitumor activity in a range of adult cancers, but has not previously been tested on pediatric cancers.[8–12] As PV-10 induced cell death in different adult cancers, has been assessed in several clinical trials,[11,13,17–19] and because Rose Bengal has previously been administered to pediatric patients to diagnose infantile jaundice without inducing any severe side effects,[6] we investigated the effects of PV-10 on different neuroblastoma cell lines. PV-10 decreased cell viability in neuroblastoma cell lines in a concentration-dependent manner. Normal fibroblast cell lines and a primary bone marrow sample were less sensitive to PV-10. These data are similar to previously published results, where concentrations of PV-10 between 100 and 200 μM were cytotoxic to colon, ovarian, and gastric cancer cell lines[8,10,12] but were not cytotoxic to normal mouse fibroblasts (NIH 3T3)[12] and indicate that PV-10 could be an effective treatment for neuroblastoma.

To characterize the target modulation of PV-10, we focused on two neuroblastoma cell lines (SK-N-AS and IMR5) with different genetic backgrounds and different tumor histories. Neuroblastoma is a genetically heterogeneous disease and the different cell lines were chosen to reflect this. The most common oncogenic drivers in neuroblastoma are *MYCN* amplification, which is seen in ~25% of patients, anaplastic lymphoma kinase (*ALK*) mutation and amplification which is seen in ~10%–15% of patients and mutations in *TP53* acquired at relapse.[2] Using the COSMIC Cell Lines Project[20] and a recently published study,[28] we identified that SK-N-AS cells have mutated neuroblastoma RAS viral oncogene homolog (*NRAS*), while IMR5 cells have copy number gain of *ALK* and *MYCN*, overexpress Akt3, and have a homozygous mutation of mechanistic target of rapamycin (*MTOR*). In addition, the SK-N-AS cell line was derived from a metastatic tumor while the IMR5 cell line was derived from a primary tumor.

By phase-contrast microscopy, we found that PV-10 was cytotoxic to neuroblastoma cells and consistent with our IC_{50} values, we identified that SK-N-AS cells were less sensitive to treatment than IMR5 cells. These data were verified by time-lapse video microscopy which again showed that SK-N-AS cells were less sensitive to treatment than IMR5 cells. Despite the differences in sensitivity to 100 μM PV-10 at early times, this concentration was still cytotoxic to most SK-N-AS cells at 96 hours and increasing the dose to 200 μM further increased SK-N-AS cell death. These data, and cytotoxicity results from the alamar blue assay using multiple cell lines from different tumors, suggest that PV-10 could be an effective treatment for all neuroblastoma, including primary, relapsed, and metastatic disease, although doses may need to be higher for some sub-types.

It has previously been shown, by multiphoton microscopy, that PV-10 acts by disrupting lysosomes in hepatoma cells, leading to cell death.[7] The disruption of lysosomes specifically affects cancer cell survival because cancer cells have an altered metabolism and can depend on lysosomes for the recycling of nutrients and removal of the products of rapid growth and division, such as aggregated proteins and damaged organelles.[29] Furthermore, disruption of lysosomes can lead to the release of cathepsin proteases, which can induce either necrosis

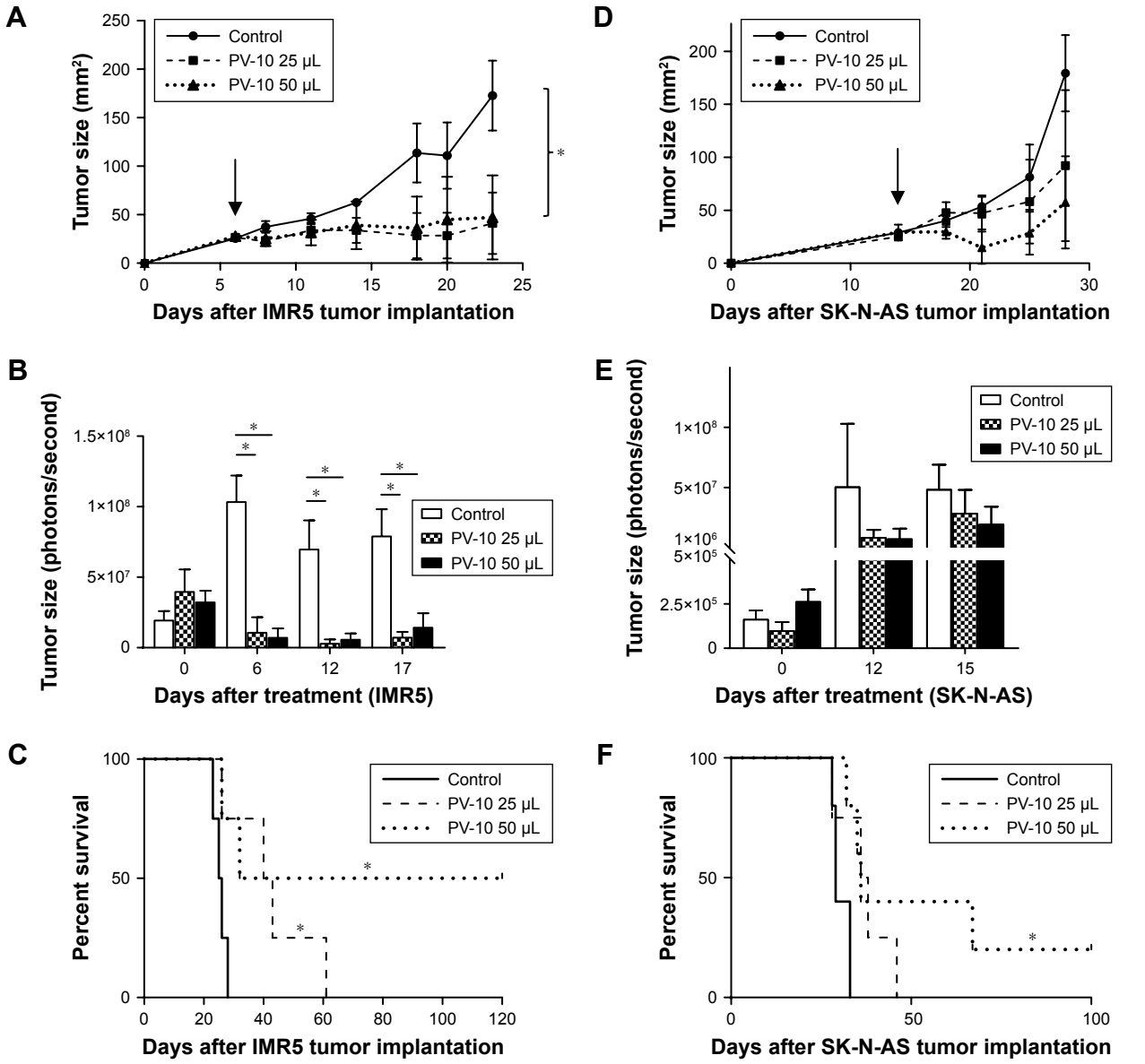

Figure 7 PV-10 induces tumor regression in vivo.

Notes: CB17 SCID mice (n=4 per group) were subcutaneously injected on the right flank with either IMR5-mCherryFluc or SK-N-AS-mCherryFluc cells. When tumor size was at least 25 mm², tumors were injected with either 50 µL PBS (vehicle control) or 25 or 50 µL PV-10. (**A**) IMR5-mCherryFluc tumor growth was measured using a Vernier caliper. Arrow indicates treatment day (day 6). Mean tumor size and standard errors of the mean are shown. Asterisks show significant differences, unpaired Student's *t*-test, $P<0.05$. (**B**) IMR5-mCherryFluc tumor growth was measured using the Xenogen IVIS 200 system to detect bioluminescent signal following intraperitoneal injection with D-luciferin. Mean tumor size and standard errors of the means are shown. Asterisks show significant differences, paired Student's *t*-test, $P<0.05$. (**C**) Survival curve for mice with IMR5-mCherryFluc tumors. Asterisks show significant differences, log-rank (Mantel-Cox) test, $P<0.05$. (**D**) SK-N-AS-mCherryFluc tumor growth was measured using a Vernier caliper. Arrow indicates treatment day (day 14). Mean tumor size and standard errors of the means are shown. No statistical significance was observed between the treatment groups. (**E**) SK-N-AS-mCherryFluc tumor growth was measured using the Xenogen IVIS 200 system to detect bioluminescent signal following intraperitoneal injection with D-luciferin. Mean tumor size and standard errors of the mean are shown. No statistical significance was observed between treatment groups. (**F**) Survival curve for mice with SK-N-AS-mCherryFluc tumors. Asterisk shows significant difference, log-rank (Mantel-Cox) test, $P<0.05$.

or apoptosis.[29] To investigate the effect of PV-10 on lysosomes in neuroblastoma, we observed cells stained with LysoTracker Green DND-26, which concentrates and fluoresces in acidic organelles. Supporting previous data,[7] we found that lysosomes appeared as distinct foci in PBS-treated SK-N-AS and IMR5 cells, but were absent in 100 µM PV-10-treated IMR5 cells and 200 µM PV-10-treated SK-N-AS cells.

Recently, in murine colon carcinoma cells (CT-26), PV-10 was shown to decrease the percentage of S phase cells and increase the percentage of G2/M phase cells, in a concentration-dependent manner.[8] Supporting these data, we found that PV-10 decreased the percentage of S phase cells, in both 100 µM PV-10-treated IMR5 cells and 200 µM PV-10-treated SK-N-AS cells. In addition, we identified

that PV-10 induced an increase in G1 phase cells in 100 µM PV-10-treated IMR5 cells and 200 µM PV-10-treated SK-N-AS cells and increased the percentage of cells in G2/M phase in 200 µM PV-10-treated SK-N-AS cells. Our results indicate that PV-10 affects the cell cycle in a time- and cell line-dependent manner.

In human adult cancer cell lines, PV-10 induces cell death by different mechanisms in a cell line-dependent manner. PV-10 induced cell death by primary necrosis in SW480 colorectal adenocarcinoma cells,[8] by a combination of apoptosis and necrosis in HCT-116 colorectal carcinoma and HT-29 colorectal adenocarcinoma cell lines,[8] and in three human primary melanoma cell samples[15] and by primarily apoptosis in UWB ovarian carcinoma cells[10] and AGS gastric adenocarcinoma cells.[12] Similar to the results using ovarian carcinoma and gastric adenocarcinoma cells, we identified that treatment with PV-10 induced apoptosis in a concentration-dependent manner in both SK-N-AS and IMR5 neuroblastoma cell lines. Our studies, alongside previously published data, suggest that while PV-10 is cytotoxic to a range of different cancers, its target modulatory effects in these cancers may be different.

Although single agent PV-10 has demonstrated efficacy in clinical trials and preclinical studies, high-risk neuroblastoma patients are treated with multiple chemotherapies and radiation following relapse.[2] We therefore investigated the potential of PV-10 in combined treatment regimens with commonly used chemotherapeutic agents. Following initial screens, we identified that a sub-cytotoxic dose of PV-10 (50 µM) was synergistic with doxorubicin, etoposide, and vincristine in both the cell lines tested (SK-N-AS and IMR5). In addition, pretreatment with PV-10 before irradiation improved the efficacy of radiation treatment for both SK-N-AS and IMR5 cells. These data are consistent with previous data where, in a Phase II clinical trial, pretreatment of adult melanoma patients with PV-10 followed by radiotherapy, induced tumor regression without a large increase in toxicity to patients.[14] Our results indicate that PV-10 could be effectively combined with different commonly used treatments, to benefit high-risk patients with relapsed neuroblastoma.

Intralesional injection of PV-10 has previously been shown to induce regression of subcutaneous syngeneic colon tumors,[8] syngeneic subcutaneous breast tumors,[9] and melanoma.[9,15] Having identified that PV-10 was cytotoxic to pediatric solid tumor cell lines in vitro, we investigated the activity of PV-10 in vivo using subcutaneous neuroblastoma xenografts in mice. Similar to previous studies, we found that pharmacologically relevant doses[13,14,18] of PV-10-induced tumor regression and increased survival in a dose- and tumor-dependent manner. Injection of 25 and 50 µL PV-10 induced early tumor regression, with 50 µL PV-10 increasing overall survival in mice with either SK-N-AS or IMR5 tumors.

Our studies provide preclinical proof-of-concept data on the efficacy of PV-10 in neuroblastoma. Mechanistically, we have found that PV-10 acts by disrupting lysosomes, inducing cell cycle changes and initiating cell death by apoptosis. We have also identified several commonly used treatments with which PV-10 shows synergistic activity. Furthermore, we have validated the efficacy of PV-10 in vivo, using neuroblastoma xenograft mouse experiments. Our experiments, carried out in representative cell lines and in vivo in immunocompromised mice, provide evidence for the direct cytotoxic potential of PV-10, as well as mechanisms by which this agent may induce target modulatory effects in cancer cells. We have also identified agents that can be combined to generate treatment synergy, providing the framework for the formulation of early phase clinical trials. This, in addition to the expected immunostimulatory effect of PV-10 described previously,[15,16] provides support for a potential approach where a PV-10 backbone regimen can be combined with agents such as immune checkpoint inhibitors to further enhance its activity in patients with relapsed or refractory neuroblastoma.

Ethical approval

The primary bone marrow sample used in this study was obtained after local Research Ethics Board approval (Ethics ID #17184) and written informed consent. All applicable international, national, and institutional guidelines for the care and use of animals were followed. All animal procedures were carried out in accordance with the guidelines of the Canadian Council on Animal Care and the NIH guidelines on the care and use of laboratory animals. All protocols were reviewed and approved by the Animal Care Committee of the University of Calgary (Protocol approval number: AC16-0243).

Data availability

The data sets generated and/or analyzed during the current study are available from the corresponding author on reasonable request.

Acknowledgments

This research study was supported by The POETIC Foundation (grant number 10014557) and Provectus Biopharmaceuticals Inc (grant number 10017458). We thank the Charbonneau Microscope Facility (University of Calgary) for support with phase-contrast and fluorescence microscopy, the Live Cell Imaging Facility (University of Calgary) for support with time-lapse video microscopy, and the University

of Calgary Flow Cytometry Facility for support with flow cytometry experiments.

An abstract of this paper was presented at the 2018 ASCO Annual Meeting as a poster presentation with interim findings, and the poster's abstract has been published.[30] Provectus Biopharmaceuticals Inc provided partial trainee research support funding for this presentation.

Disclosure

The authors report no conflicts of interest in this work.

References

1. Chen X, Pappo A, Dyer MA. Pediatric solid tumor genomics and developmental pliancy. *Oncogene*. 2015;34(41):5207–5215.
2. Moreno L, Caron H, Geoerger B, et al. Accelerating drug development for neuroblastoma – new drug development strategy: an innovative therapies for children with cancer, European network for cancer research in children and adolescents and international society of paediatric oncology Europe neuroblastoma project. *Expert Opin Drug Discov*. 2017;12(8):1–11.
3. Cheung NK, Dyer MA. Neuroblastoma: developmental biology, cancer genomics and immunotherapy. *Nat Rev Cancer*. 2013;13(6):397–411.
4. Park JR, Bagatell R, London WB, et al. Children's Oncology Group's 2013 blueprint for research: neuroblastoma. *Pediatr Blood Cancer*. 2013;60(6):985–993.
5. Maker AV, Prabhakar B, Pardiwala K. The potential of intralesional rose Bengal to stimulate T-cell mediated anti-tumor responses. *J Clin Cell Immunol*. 2015;6(4):343.
6. Yvart J, Moati F, Alvarez F, Odievre M, Desgrez A. 131I rose Bengal: its use in the evaluation of infantile jaundice. *Eur J Nucl Med*. 1981;6(8):355–359.
7. Wachter EA, Dees C, Harkins J, Fisher WG, Scott T. Functional imaging of photosensitizers using multiphoton microscopy. In: Periasamy A, So PTC, editors. *Proceedings of SPIE, Multiphoton Microscopy in the Biomedical Sciences II*. Vol. 4620. Bellingham, WA: International Society for Optics and Photonics; 2002:143–147.
8. Qin J, Kunda N, Qiao G, et al. Colon cancer cell treatment with rose Bengal generates a protective immune response via immunogenic cell death. *Cell Death Dis*. 2017;8(2):e2584.
9. Toomey P, Kodumudi K, Weber A, et al. Intralesional injection of rose Bengal induces a systemic tumor-specific immune response in murine models of melanoma and breast cancer. *PLoS One*. 2013;8(7):e68561.
10. Koevary SB. Selective toxicity of rose Bengal to ovarian cancer cells in vitro. *Int J Physiol Pathophysiol Pharmacol*. 2012;4(2):99–107.
11. Thompson JF, Hersey P, Wachter E. Chemoablation of metastatic melanoma using intralesional rose Bengal. *Melanoma Res*. 2008;18(6):405–411.
12. Zamani Taghizadeh Rabe S, Mousavi SH, Tabasi N, et al. Rose Bengal suppresses gastric cancer cell proliferation via apoptosis and inhibits nitric oxide formation in macrophages. *J Immunotoxicol*. 2014;11(4):367–375.
13. Thompson JF, Agarwala SS, Smithers BM, et al. Phase 2 study of intralesional PV-10 in refractory metastatic melanoma. *Ann Surg Oncol*. 2015;22(7):2135–2142.
14. Foote M, Read T, Thomas J, Wagels M, Burmeister B, Smithers BM. Results of a phase II, open-label, non-comparative study of intralesional PV-10 followed by radiotherapy for the treatment of in-transit or metastatic melanoma. *J Surg Oncol*. 2017;115(7):891–897.
15. Liu H, Innamarato PP, Kodumudi K, et al. Intralesional rose bengal in melanoma elicits tumor immunity via activation of dendritic cells by the release of high mobility group box 1. *Oncotarget*. 2016;7(25):37893–37905.
16. Liu H, Weber A, Morse J, et al. T cell mediated immunity after combination therapy with intralesional PV-10 and blockade of the PD-1/PD-L1 pathway in a murine melanoma model. *PLoS One*. 2018;13(4):e0196033.
17. Lippey J, Bousounis R, Behrenbruch C, et al. Intralesional PV-10 for in-transit melanoma-A single-center experience. *J Surg Oncol*. 2016;114(3):380–384.
18. Ross MI. Intralesional therapy with PV-10 (rose Bengal) for in-transit melanoma. *J Surg Oncol*. 2014;109(4):314–319.
19. Read TA, Smith A, Thomas J, et al. Intralesional PV-10 for the treatment of in-transit melanoma metastases-Results of a prospective, non-randomized, single center study. *J Surg Oncol*. 2018;117(4):579–587.
20. Catalogue of Somatic Mutations in Cancer (COSMIC). Available from: https://cancer.sanger.ac.uk/cosmic. November 20, 2018.
21. American Type Culture Collection. Available from: www.atcc.org. Accessed November 20, 2018.
22. George RE, Sanda T, Hanna M, et al. Activating mutations in ALK provide a therapeutic target in neuroblastoma. *Nature*. 2008;455(7215):975–978.
23. Huang R, Cheung NK, Vider J, et al. MYCN and Myc regulate tumor proliferation and tumorigenesis directly through Bmi1 in human neuroblastomas. *Faseb J*. 2011;25(12):4138–4149.
24. Goldschneider D, Horvilleur E, Plassa LF, et al. Expression of C-terminal deleted p53 isoforms in neuroblastoma. *Nucleic Acids Res*. 2006;34(19):5603–5612.
25. Jayanthan A, Ruan Y, Truong TH, Narendran A. Aurora kinases as druggable targets in pediatric leukemia: heterogeneity in target modulation activities and cytotoxicity by diverse novel therapeutic agents. *PLoS One*. 2014;9(7):e102741.
26. Chou TC. Drug combination studies and their synergy quantification using the Chou-Talalay method. *Cancer Res*. 2010;70(2):440–446.
27. Lun X, Ruan Y, Jayanthan A, et al. Double-deleted vaccinia virus in virotherapy for refractory and metastatic pediatric solid tumors. *Mol Oncol*. 2013;7(5):944–954.
28. Hart LS, Rader J, Raman P, et al. Preclinical therapeutic synergy of MEK1/2 and CDK4/6 inhibition in neuroblastoma. *Clin Cancer Res*. 2017;23(7):1785–1796.
29. Fennelly C, Amaravadi RK. Lysosomal biology in cancer. *Methods Mol Biol*. 2017;1594:293–308.
30. Swift L, Zhang C, Trippett TM, Narendran A. In vitro and xenograft anti-tumor activity, target modulation and drug synergy studies of PV-10 against refractory pediatric solid tumors [poster abstract]. *J Clin Oncol*. 2018;36(15 suppl):10557.